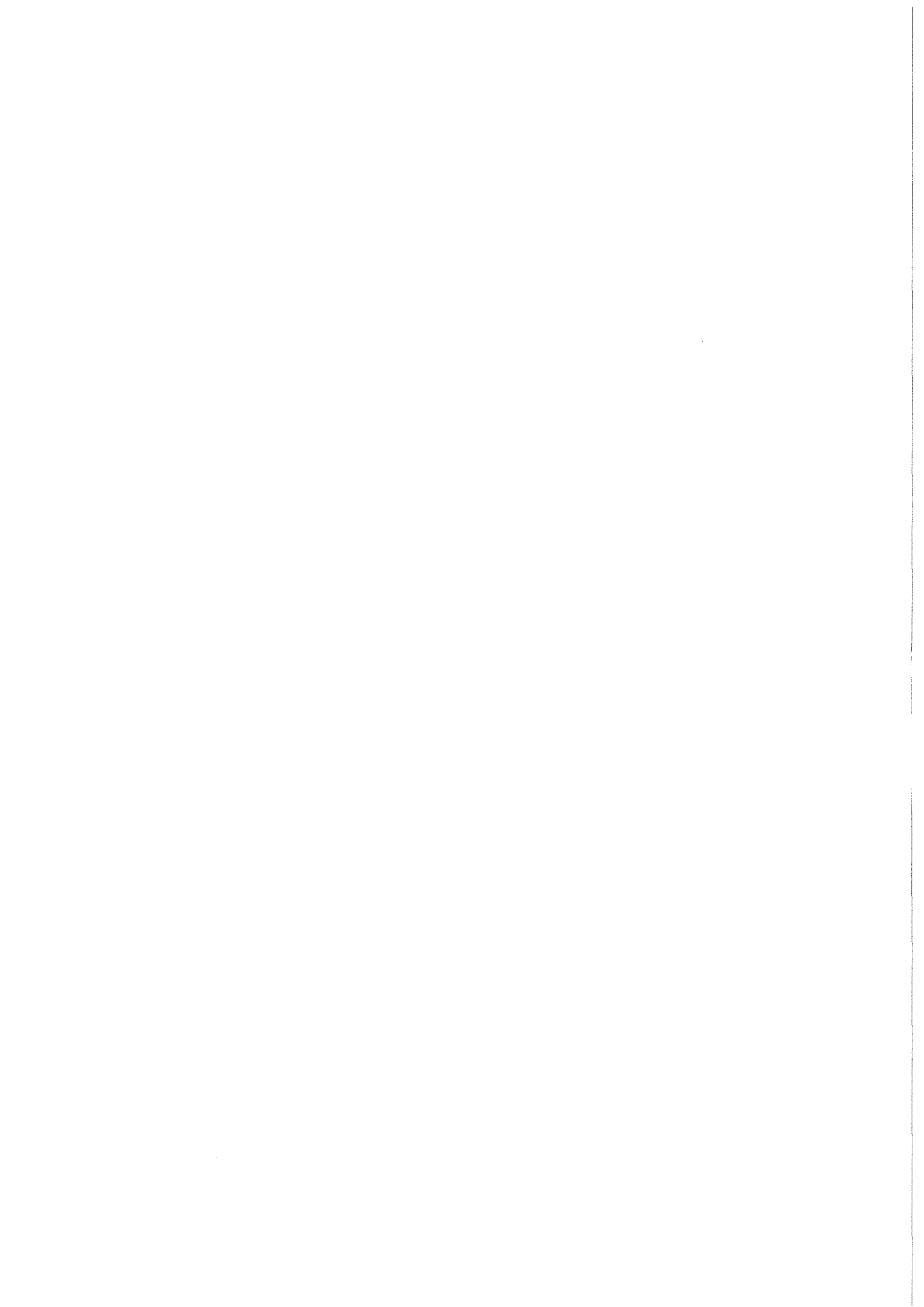


KfK 3465
Februar 1983

Basis and Concepts for the Electromagnetic Acceleration of Pellets for Injection into Inertial Confinement Fusion Reactor Chambers

R. Kreuz
Institut für Neutronenphysik und Reaktortechnik

Kernforschungszentrum Karlsruhe



KERNFORSCHUNGSZENTRUM KARLSRUHE

Institut für Neutronenphysik und Reaktortechnik

KfK 3465

Basis and Concepts for the
Electromagnetic Acceleration
of Pellets for Injection into
Inertial Confinement Fusion Reactor Chambers

R. Kreuz⁺⁾

⁺⁾ INTERATOM, Internationale Atomreaktorbau GmbH,
Bergisch Gladbach

Kernforschungszentrum Karlsruhe GmbH, Karlsruhe

Als Manuskript vervielfältigt
Für diesen Bericht behalten wir uns alle Rechte vor

Kernforschungszentrum Karlsruhe GmbH
ISSN 0303-4003

Summary

The possibility of the electromagnetic acceleration of pellets for injection into inertial confinement fusion reactor chambers is investigated. The acceleration by a high gradient magnetic field is discussed for different types of driving bodies (non-ferromagnetic cylinder, ferromagnetic cylinder, superconducting coil) of the pellet carrier. Two accelerator concepts are described. Alternatively, pellet acceleration by a railgun is investigated. In all cases a 1 g-projectile can be accelerated to a reference velocity of 200 m/s over a distance of the order of 1 m which corresponds to an acceleration time of the order of 10 ms. For each of the methods investigated reference parameter lists are given as a basis of orientation for the technical design of an electromagnetic pellet accelerator.

Grundlagen und Konzepte zur elektromagnetischen Beschleunigung von Pellets für die Injektion in Trägheitsfusions-Reaktorkammern

Zusammenfassung:

Es wird die Möglichkeit der elektromagnetischen Beschleunigung von Pellets zur Injektion in Reaktorkammern für die Trägheitsfusion untersucht. Für verschiedene Treibkörperarten (nicht-ferromagnetischer Zylinder, ferromagnetischer Zylinder, supraleitende Spule) des Pelletträgers werden die Beschleunigung durch ein Magnetfeld mit großem Gradienten behandelt und zwei Beschleunigerkonzepte beschrieben. Zum anderen wird die Pelletbeschleunigung nach dem Schienengeschütz-Prinzip untersucht. In allen Fällen kann eine Projektilmasse von einigen Gramm auf eine Referenz-Geschwindigkeit von 200 m/s über eine Strecke von der Größenordnung 1 m beschleunigt werden, was einer Beschleunigungszeit in der Größenordnung von 10 ns entspricht. Für jede der untersuchten Beschleunigungsmethoden wird ein Satz von Referenzparameterwerten als Orientierungsbasis für eine technische Ausführung eines elektromagnetischen Pellet-Beschleunigers angegeben.

Table of Contents

	<u>Page</u>	
I	Introduction	1
II	Acceleration by a High Gradient Magnetic Field	3
II.1	Introduction	3
II.2	Projectile Acceleration	6
II.2.1	Non-ferromagnetic Cylinder	6
II.2.1.1	Acceleration Distance	6
II.2.1.2	Example	7
II.2.1.3	Cylinder Heating	8
II.2.1.4	Reference Parameters	10
II.2.2	Ferromagnetic Cylinder	12
II.2.2.1	Acceleration Distance	12
II.2.2.2	Gradient of Magnetic Induction of the Field Coil	13
II.2.2.3	Pellet Carrier Reference Design	15
II.2.2.4	Discussion of the Acceleration Distance	18
II.2.2.5	Reference Parameters	19
II.2.3	Superconducting Coil	22
II.2.3.1	Acceleration Distance	22
II.2.3.2	Discussion of the Acceleration Distance	24
II.2.3.3	Reference Parameters	29
II.3	Types of Accelerator	32
II.3.1	Single Coil Operation	32
II.3.2	Traveling Magnetic Wave Accelerator	35
II.3.2.1	Functioning Principle	35
II.3.2.2	Accelerator Scheme	35
II.3.2.3	Energy Stored per Coil Turn	38
II.4	Conclusion	39
III	Railgun Accelerator	41
III.1	Introduction	41
III.2	Principle of Acceleration	41
III.3	Electric Circuit	43
III.4	Projectile Acceleration	44
III.4.1	Inductance of the Railgun	45
III.4.2	Acceleration Distance	46
III.5	Rail Heatup	48
III.6	Reference Parameters	51

I Introduction

Energy generation by means of inertial confinement fusion of light atomic nuclei requires that fuel pellets filled with fusionable material are brought into a reaction chamber with high precision and at a frequency of some Hz, where they are exposed to high-intensity concentrated laser or particle radiation. The pellet injection velocity should be between 100 and 1000 m/s.

Various methods can be considered for pellet acceleration: acceleration by a high pressure gas or by electric or magnetic fields. Within the framework of a reactor study on inertial confinement fusion by means of heavy ion beams (HIBALL) the possibility of pneumatic pellet injection was studied [1]. In this work the fundamentals are treated of several possibilities of electromagnetic pellet acceleration. In all cases the pellet is accelerated in an indirect way, i.e., by means of a pellet carrier, on which the acceleration forces act. Direct acceleration, e.g., of a pellet with metallic external layer in an inhomogeneous magnetic field, would heat up the pellet by induced currents. This is not favorable if cryogenic pellets with a solid inner deuterium/tritium layer are used such as e.g. for the HIBALL system.

Under the topic of projectile acceleration by a high gradient magnetic field, discussed in Chapter II, the influence of various driving bodies (non-ferromagnetic cylinder, ferromagnetic cylinder, superconducting coil) of the pellet carrier on the acceleration distance are treated and expressions derived to describe the dependence of the accelerating distance on the intensity and gradient of the accelerated magnetic field. Two acceleration concepts are described. In Chapter III pellet acceleration by means of the railgun method is treated as an alternative.

This paper has been written to serve above all as a parameter study on the feasibility of electromagnetic acceleration of masses of the order of grams under different acceleration concepts. The reference parameter sets indicated for each concept apply to the reference pellet velocity of 200 m/s chosen for HIBALL and are intended as providing a basis for the selection of a suitable electromagnetic pellet accelerator for a HIBALL reactor chamber as an alternative to pneumatic pellet acceleration.

II Acceleration by a High Gradient Magnetic Field

II.1 Introduction

The acceleration treated below of pellets to be injected into reactor chambers in order to bring about inertial confinement fusion relies on the following principle:

If a metallic body with a magnetic moment is in an inhomogeneous magnetic field, it is exposed to a force whose size depends both on the physical properties of the body and on the nature of the magnetic field. Table II.1-1 is a listing of the expressions valid for the forces which appear when

- i) a metallic, non-ferromagnetic cylinder is in the magnetic field of a circular coil (provided the stay time is short as compared with the time of permeation of the magnetic field into the cylinder);
- ii) a ferromagnetic cylinder with a magnetic moment (as a result of an external magnetic field or permanently) is in the inhomogeneous magnetic field of a circular coil;
- iii) a ring of superconducting material with a magnetic moment (as a result of a current induced by cooling down in a magnetic field to less than the critical temperature of the superconductor: flux entrapment) is in an inhomogeneous magnetic field of a circular coil.

Accelerated Body	Accelerating Force	Parameter
Cylinder made from conducting material (e.g. copper)	$F = \frac{B^2}{2\mu_0} \pi r_c^2$	r_c : radius of cylinder B : magnetic induction of field coil
<p>Generally, the force $F = \vec{M} (\vec{\nabla} B)$ acts on a magnetic dipole moment \vec{M} in a magnetic field with a gradient $\vec{\nabla} B$. If the dipole moment is given by a ferromagnetic cylinder or by a current-carrying conductor loop, the following specific setups are obtained (\vec{M} parallel to the x-direction, cylindrically symmetric problem):</p>		
Cylinder made from ferromagnetic material	$F = \mathcal{M}_c V_c \delta_x B$	$\delta_x B$: gradient of B in the x-direction \mathcal{M}_c : magnetization of ferromagnetic cylinder (dipole moment per unit of volume) V_c : cylinder volume
Current-carrying conductor loop (superconducting coil)	$F = \pi r_c^2 I \delta_x B$	I : current intensity in conductor loop r_c : radius of conductor loop

Table II.1-1: Setups for the acceleration forces acting on various bodies in a magnetic field with magnetic induction B and gradient $\delta_x B$ (cylindrical symmetry).

For electromagnetic pellet injection such bodies can be inserted in a carrier, which on its front side, i.e., in the direction of acceleration, carries the pellet; see Fig. II.1-1.

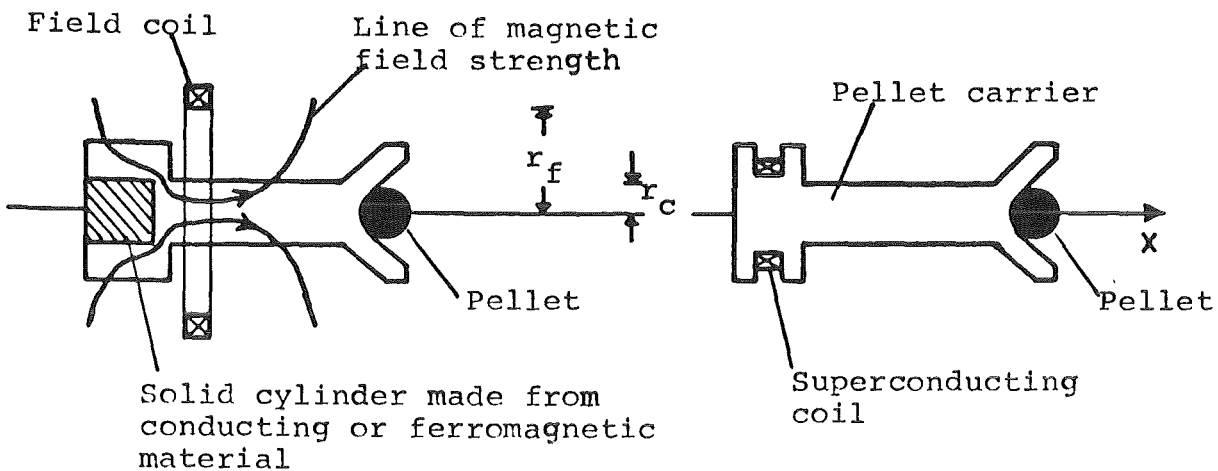


Fig. II.1-1: Schematic representation of pellet carrier with different driving bodies in the magnetic field of a circular coil.

However, the accelerating effect of the magnetic field of a current-carrying conductor loop is really effective only over a distance from the loop center corresponding in size to the radius of the conductor loop. Therefore, an accelerator serving the purpose discussed here will, in principle, consist of a set of circular coils in series. The pellet carrier moves in a guide tube in the interior of the coil set.

From the equations of forces in Table II.1-1 and assuming a uniformly accelerated movement, i. e. a constant gradient of magnetic induction of the field coils, expressions are derived for the acceleration distances as a function of the parameters specific for the driving bodies and the field coils. Sets are indicated of real parameter values, especially on the projectile structure and on field coil dimensioning, for a pellet reference velocity of 200 m/s; see Section II.2. Finally, in Section II.3 two possible accelerator concepts are described.

II.2 Projectile Acceleration

II.2.1 Non-ferromagnetic Cylinder

This approach has the drawback that the non-ferromagnetic material while accelerated is heated up by the induced current generating the magnetic moment; this is not favorable if the requirement is for a cryogenic pellet. For the sake of completeness this case, inclusive of an estimate of cylinder heating, is also taken into account. If applicable, a suitable thermal insulation must be provided between the driving body and the pellet.

II.2.1.1 Acceleration Distance

Setup for the acceleration force provided that the time of permeation of the magnetic field is long as compared with the time of acceleration and, moreover, the magnetic field gradient is sufficiently high so that the magnetic field pressure at the cylinder rear end is small compared with the magnetic field pressure at the cylinder front end:

$$F = \frac{B^2}{2\mu_0} \pi r_c^2$$

B: magnetic induction of the
field coil on the coil axis

r_c : radius of cylinder

μ_0 : magnetic permeability in the
vacuum

Projectile acceleration:

$$a = \frac{\pi B^2 r_c^2}{2\mu_0 M}$$

M: projectile mass

Acceleration distance:

$$l_a = \frac{v^2}{2a} = \frac{\mu_0}{\pi} v^2 \frac{M}{B^2 r_c^2}$$

v: projectile velocity

II.2.1.2 Example

$$v = 200 \text{ m/s}$$

$$r_c = 3 \text{ mm}$$

$$\mu_0 = 1.26 \times 10^{-6} \text{ Vs/Am}$$

Consequently, the relation holds:

$$l_a [\text{m}] = 1.78 \times 10^3 \frac{M [\text{kg}]}{B^2 [\text{T}^2]}$$

If $M = 3\text{g}$, we obtain:

B [T]	1	1.6	2.3
l_a [m]	5.4	2	1
a [m/s ²] (acceleration)	3.7×10^3	10^4	2×10^4
t_a [ms] (time of acceleration)	54	20	10

Table II.2-1: Acceleration distance for pellet acceleration by means of a non-ferromagnetic cylinder as a function of the magnetic induction B of the field coils

The 3g projectile mass could e.g. be subdivided as follows:
A copper cylinder of 3 mm radius and 6 mm length has a mass of 1.6 g. If the pellet has a mass of 0.35 g [1], about 1 g is left for the pellet carrier mass, i.e., in case plastic material of 1 g/cm³ density is used, the volume of the pellet carrier material is about 1 cm³.

II.2.1.3 Cylinder Heating

Setup for the energy loss resulting from the electric resistance:

$$E_e = R_c \cdot I_c^2 t_a$$

R_c : electric resistance of cylinder material

I_c : induced current on cylinder surface

t_a : time of acceleration up to velocity v

The following relations hold:

$$t_a = \frac{v}{a} = v \frac{2\mu_0 M}{\pi B^2 r_c^2}$$

$$I_c = \frac{2 B r_c}{\mu_0}$$

, Argument:

"External" magnetic induction can be thought of as being compensated by an opposed induction of the same amount and generated in the cylinder by a circular current I_c with the radius r_c [2].

In an approximation, the following setup is written for the electric resistance R_c [2]:

$$R_c = \rho_c \frac{2\pi r_c/2}{r_c l_c} = \rho_c \frac{\pi}{l_c}$$

ρ_c : resistivity of cylinder material (in Ω m)

l_c : length of cylinder

r_c : radius of cylinder

This gives:

$$E_e = \frac{8}{\mu_0} v M \frac{\rho_c}{l_c}$$

Example:

$$v = 200 \text{ m/s}$$

$$M = 3 \text{ g}$$

$$l_c = 2r_c = 6 \text{ mm}$$

} see Table II.2-2

Copper: $\rho_c \approx 1 \times 10^{-10} \Omega \text{ m}$ (upper limit at 20 K)

This gives:

$$E_e = 0.064 \text{ J} \quad [t_a = 20 \text{ ms} \Rightarrow p_e = 3.2 \text{ W}]$$

The associated temperature rise in the cylinder can be calculated as follows:

$$\Delta T = T_2 - T_1$$

T_1 : initial temperature

T_2 : end temperature

Deduction of T_2 :

$$E_e = M_c \cdot \int_{T_1}^{T_2} C_v(T) dT$$

C_v : specific heat of cylinder material

$$\text{With } C_v(T) = a_c T^3$$

a_c : constant

the following general expression is obtained:

$$T_2 = \left[\frac{4 E_e}{M_c a_c} - T_1^4 \right]^{\frac{1}{4}}$$

In the particular case of $E_e = 0.064 \text{ J}$, $M_c = 1.6 \text{ g}$,
 $a_c = 8.4 \times 10^{-7} \text{ J/gK}^4$ *) and $T = 5 \text{ K}$, we obtain $T_2 = 21 \text{ K}$.

*) can be deduced from data in [3].

No optimization is made here, especially not with a view to reducing the cylinder end temperature, because pellet acceleration by means of a ferromagnetic cylinder as discussed below is better suited which is not accompanied by intrinsic cylinder heating.

II.2.1.4 Reference Parameters

The reference parameter set given in Table II.2-2 is based on a copper cylinder of the mass 1.6 g and on a projectile mass of 3 g.

For the choice of the length of acceleration time the time of permeation of the external magnetic field into the driving body cylinder must be taken into account. To do this, the calculations carried out in [14] on the temperature diffusion in a cylinder can be transferred to the diffusion of a magnetic field under analogous boundary conditions, with $\kappa = \rho_c / \mu_0$ being the variable analogous to thermal diffusivity (unit m^2/s). The dimensionless variable $K = \rho_c t / \mu_0 r_c^2$ is decisive for the distribution of the magnetic field in the cylinder after the time of exposure t . If for the time of acceleration (time of exposure to the magnetic field of the field coils) a reference value of 10 ms is taken, a K -value of 0.09 is obtained for a resistivity ρ_c of $1 \times 10^{-10} \Omega \text{ m}$ (copper at 5 K) and a cylinder radius r_c of 3 mm. According to [14] a magnetic field intensity of about 10% of that prevailing on the cylinder surface is then obtained in the center of the cylinder.

The acceleration distance of 1 m indicated in Table II.2-2 does not yet take into account the attenuation of the acceleration force due to the permeation of the magnetic field. To attain the reference velocity of 200 m/s within 10 ms over a distance of 1 m, the value given here for the magnetic induction of the field coils would have to be increased accordingly.

Pellet velocity	v	200 m/s
Projectile:		
total mass	M	3 g
mass of driving body (copper cylinder)	M_C	1.6 g
cylinder radius of driving body	r_C	3 mm
length of driving body	l_C	6 mm
pellet carrier mass	M_T	1.05 g
pellet mass	M_P	0.35 g
Field coils:		
magnetic induction		
- mean value, efficient in terms of acceleration (on the axis)	B	2.3 T
- maximum value, in the center of the coil	B_O	3.3 T
radius	r_f	1 cm
current intensity (to generate B_O)	I_f	52 kA
coil spacing		1 cm
coil number		100
Acceleration distance	l_a	1 m
Time of acceleration	t_a	10 ms
Driving body heating:		
heatup energy	E_e	0.064 J
initial temperature	T_1	5 K
end temperature	T_2	21 K

Table II.2-2: Reference parameter values for a projectile acceleration to 200 m/s by means of a cylindrical driving body made of copper

II.2.2 Ferromagnetic Cylinder

The acceleration of a ferromagnetic body with a magnetic moment carries the advantage that no intrinsic heating is coupled with the presence of the magnetic moment. Both ferromagnetic material classes can be considered: materials with a high but nonpermanent saturation magnetization and permanent magnets.

It is assumed that the ferromagnetic cylinder is accelerated by pulling it into the magnetic field of the field coil so that cylinder magnetization is aligned with the magnetic field of the field coil.

II.2.2.1 Acceleration Distance

Setup for the acceleration force:

$$F = \mathcal{M}_C \cdot V_C \cdot \delta_x B$$

\mathcal{M}_C : magnetic dipole moment per unit of volume of ferromagnetic cylinder in $A \ m^{-1}$ ($\mu_0 \mathcal{M}_C$: magnetization in $V \ s \ m^{-2}$)

V_C : cylinder volume

B : magnetic induction of external magnetic field

$\delta_x B$: gradient of B in the x-direction

The following expression holds:

$$\mathcal{M}_C = \frac{B_C}{\mu_0} - H$$

B_C : magnetic induction in ferromagnetic cylinder

H : field intensity of external magnetic field

In a ferromagnetic material $H \ll B_C / \mu_0$ which means that:

$$\mathcal{M}_C = \frac{B_C}{\mu_0}$$

This gives:

projectile acceleration:

$$a = \frac{B_c V_c}{\mu_0 M} \delta_x B$$

acceleration distance:

$$l_a = \frac{v^2}{2a} = \frac{v^2 \mu_0 M}{2 V_c B_c \delta_x B}$$

v = projectile velocity (at the end of acceleration)

acceleration time:

$$t_a = \frac{2 l_a}{v}$$

II.2.2.2 Gradient of Magnetic Induction of the Field Coil

For the expressions derived below for the acceleration distance the magnetic field of the accelerating field coils is approximated by the magnetic field of a circular current.

According to [4] (graphic representation in Fig. II.2-1), the following holds:

$$\frac{B(x)}{B_0} = \left[1 + \left(\frac{x}{r_f} \right)^2 \right]^{-\frac{3}{2}}$$

B(x): magnetic induction on coil axis at distance x from the coil center

B₀ is the magnetic induction in the center of the coil:

$$B_0 = \frac{\mu_0 I}{2 r_f}$$

I : coil current
r_f : coil radius

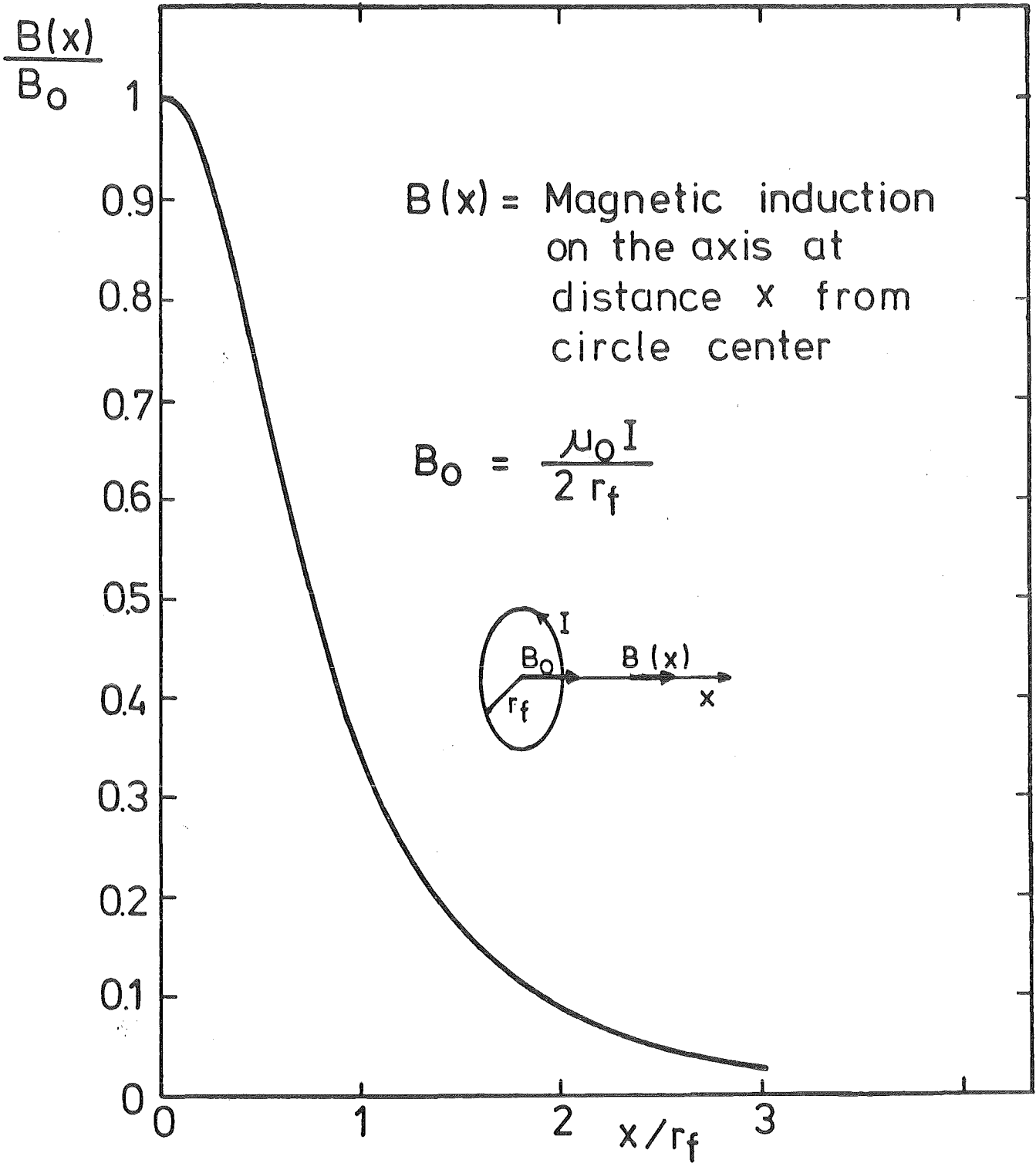


Fig. II.2-1: Magnetic induction of a circular current on the axis of the circle as a function of distance x from the center of the circle.

The expression below holds for $x/r_f = 1$:

$$\frac{B(r_f)}{B_0} \approx 35\%, \text{ i.e. } B(r_f) \approx B_0 \cdot \frac{1}{e}$$

which means that $|\delta_x B|$ essentially adopts the order of magnitude B_0/r_f within the range $0 \leq |x| \leq r_f$. For this range between the center of the coil and a distance r_f on the coil axis the expression $|\delta_x B| = 0.7 B_0/r_f$ can be written in an approximation as constituting the mean value. In the expressions defining the acceleration distance discussed in the following Sections II.2.2.4 and II.2.3.2 it is assumed that the accelerating individual coils (or the coil turns in a traveling magnetic wave accelerator) have been arranged with a spacing r_f so that, on an average, a gradient $\delta_x B$ with the amount of $0.7 B_0/r_f$ can be used for calculation over the whole acceleration distance.

II.2.2.3 Pellet Carrier Reference Design

Since the mass ratio M/M_c is included in the expression for the acceleration distance, it is appropriate to show by way of example the distribution of mass among the individual components of the projectile:

The relation below holds:

$$M = M_c + M_p + M_T$$

M_p is the pellet mass and M_T is the mass of the pellet carrier into which the ferromagnetic cylinder of mass M_c is introduced (see Fig. II.1-1).

To minimize the acceleration distance, the ratio M/M_c should be likewise minimized. On the other hand, it would be reasonable to leave a sufficiently great spacing between the pellet and the driving body so that the pellet is only little influenced by the magnetic field of the field coil; induction heating of the pellet - which, similar to the HIBALL pellet, may have a

metallic outer shell - should be largely avoided. To attain the most effective possible pellet shielding against the accelerating magnetic field, a metallic tunnel-shaped sheet metal could be provided between the pellet and the driving body (near the pellet). This is not included in the considerations in this context because the following computation is to furnish only a first reference value for the mass ratio M/M_C .

In the following considerations it is solely assumed that the spacing between the pellet and the center of the driving body is greater than the diameter of the field coil. Since the driving body is to be accelerated by pulling it into the magnetic field of a field coil, the pellet is already at the beginning of acceleration outside the zone of major efficiency *) of the accelerating field coil.

To be able to indicate a value for the mass of the pellet carrier with its relatively complicated geometry, the volume of the pellet carrier material is approximated by a cylinder volume; see Fig. II.2-2.

$$V_T = \pi \tilde{r}_T^2 \tilde{l}_T$$

\tilde{r}_T = radius of fictitious
pellet carrier volume

\tilde{l}_T = length of fictitious pellet
carrier volume.

*) see Section II.2.2.2: zone of major efficiency of
acceleration: $|x| \leq r_f$

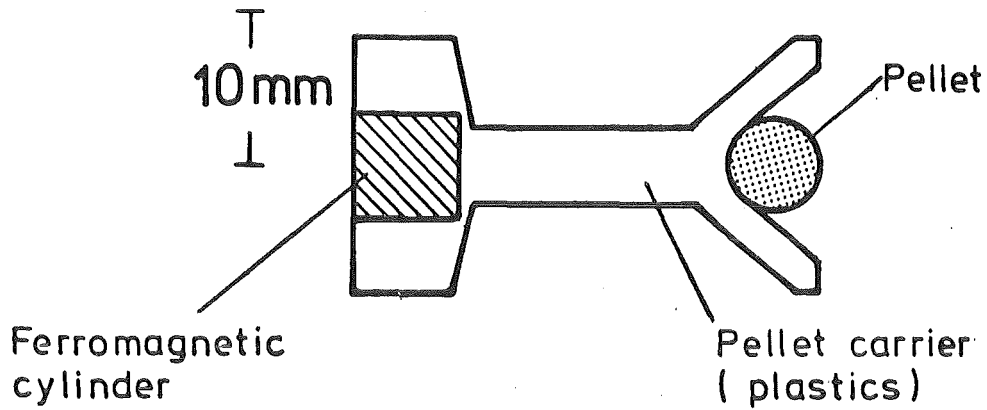


Fig. II.2-2: Pellet carrier design for electromagnetic pellet acceleration by means of a ferromagnetic cylinder; $M/M_C = 2$ (see text).

The following specific relation shall hold for the volume of the driving body:

$$V_C = \pi r_C^2 2r_C = 2 \pi r_C^3$$

Consequently:

$$M_C = 2 \pi \rho_F r_C^3$$

$$M_T = \pi \rho_T \tilde{r}_T^2 \tilde{l}_T$$

Taking into account a reference value for the radius of the field coil of 10 mm ^{*)}, the following dimensions are chosen: $r_C = 3.5$ mm; $\tilde{r}_T = 5$ mm and $\tilde{l}_T = 24$ mm, see Fig. II.2-2.

If one chooses a mass density ρ_F of 8.3 g/cm^3 (Permendur) and for the pellet carrier a synthetic material with the mass density 1 g/cm^3 (order of magnitude) one finally obtains:

$M_C = 2.25$ g and $M_T = 1.9$ g. With $M_P = 0.35$ g according to [1] we obtain $M = 4.5$ g so that the mass ratio is $M/M_C = 2$.

^{*)} reasonable value, since according to [1] the pellet radius shall be 3 mm.

II.2.2.4 Discussion of the Acceleration Distance:

The following derivation was made (see above):

$$l_a = \frac{v^2 \mu_o M}{2 V_c B_c \delta_x B}$$

It is appropriate that $m = \frac{M}{M_c}$ i.e. M is a multiple of M_c .

This gives with $\rho_f = M_c/V_c$ (specific density of the ferromagnetic material):

$$l_a = \frac{\mu_o}{2} v^2 \frac{m \rho_f}{B_c} \frac{1}{\delta_x B}$$

In Table II.2-3 the specific densities, saturation magnetizations and remanences, respectively, and the field intensities upon attainment of the saturation magnetizations have been entered for some ferromagnetic materials.

Ferromagnetic Material	ρ_f [g/cm ³]	B_c [T]	$\frac{\rho_f}{B_c}$ [$\frac{kg}{T m^3}$]	H_s [Oe]
Iron (99.91%)	7.88	2.15	3665	~1000
Permendur (50 Fe/50 Co)	8.3	2.45	3387	~ 500
78-Permalloy (78 Ni/21 Fe)	8.6	1.07	8037	~ 6
Permanent magnets:				
Carbon steel	7.75	1.0	7748	
Alnico V (Fe/Al/Ni/Co/Cu)	7.3	1.25	7306	

Table II.2-3: Material and magnetization parameters for ferromagnetic materials according to [5 and 6].

In Fig. II.2-3 the dependence is plotted of the acceleration distance l_a on the gradient $\delta_x B$ of the field coils for two values of ρ_f/B_c (Permendur, Alnico V), where $M = 2 M_c$, i.e., $m = 2$.

To achieve a projectile velocity of 200 m/s over an acceleration distance of the order of 1 m, gradients $\delta_x B$ are required of the order of 100 T/m. If one assumes a radius of 3 mm for the pellet to be accelerated [1], a radius of the field coil of the order of 1 cm is recommended. According to considerations made in Section II.2.2.2 the magnetic induction in the center of the coil is consequently of the order of 1 T. At a distance r_f of the coil center the magnetic induction is in this case still above 0.3 T, which corresponds to a magnetic field intensity of about 3×10^3 Oe. Many of the conventional ferromagnetic materials attain more than 90% of their saturation magnetization already above 10 Oe. Especially the materials listed in Table II.2-3 attain up to 10^3 Oe the values of magnetization indicated. This means that the ferromagnetic materials under consideration always remain in the state of saturation when accelerated by coils at a distance r_f (coil radius) and with a magnetic induction of the order of 1 T in the center of the coil.

II.2.2.5 Reference Parameters

The point of departure are a projectile mass of 4.5 g and a driving body made from Permendur^{*)}, mass 2.25 g, and field coils with a radius of 1 cm. With a projectile velocity of 200 m/s at the end of an acceleration distance of 1 m length 100 coils spaced 1 cm with respect to each other are consequently required, the gradient for magnetic induction being 170 T/m; see Fig. II.2-3.

^{*)} The material costs will count less if frequent reuses of the pellet carrier are provided for; see Section II.3 .

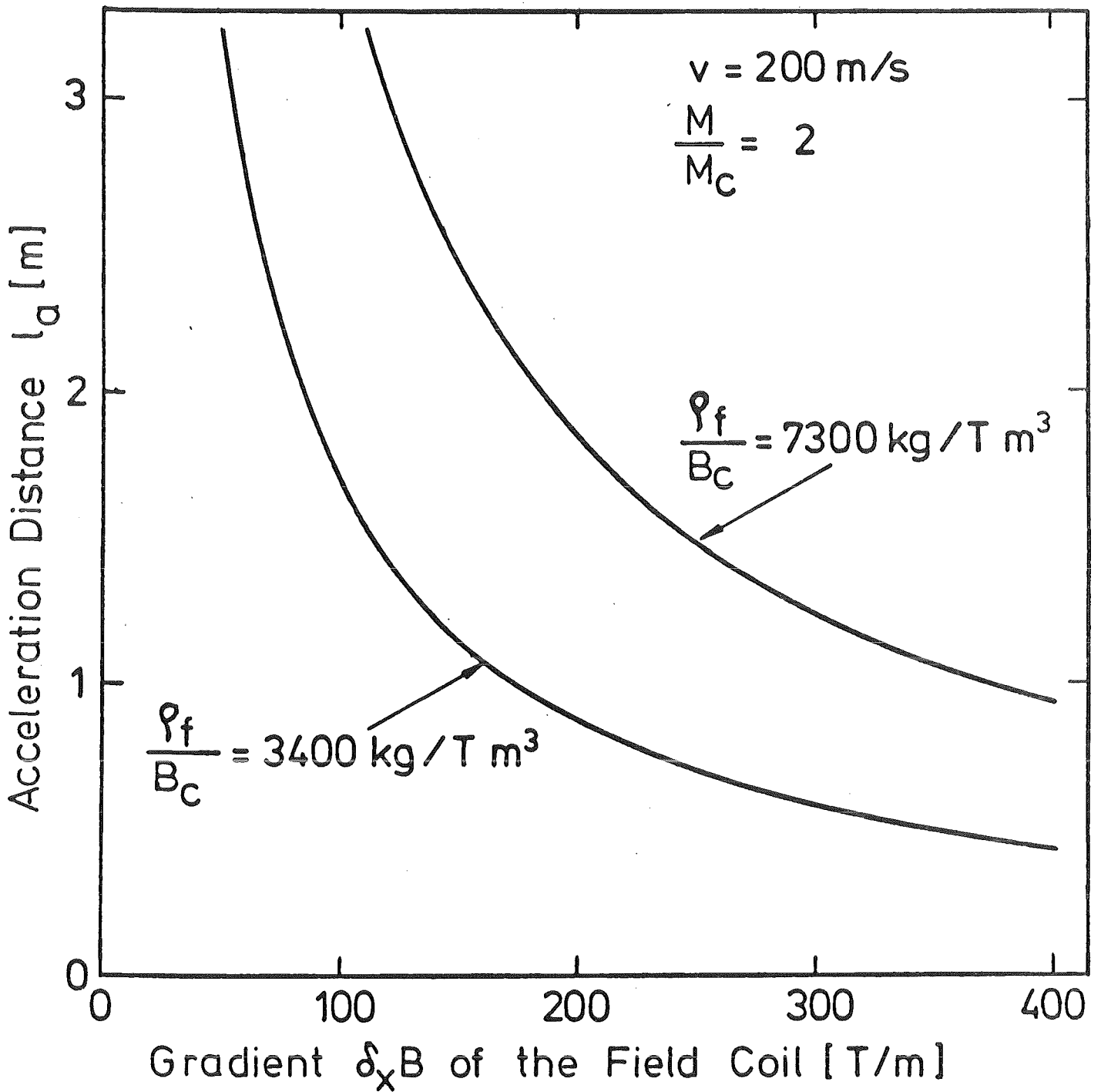


Fig. II.2-3: Acceleration distance as a function of the gradient of magnetic induction of the accelerating magnetic field for various ferromagnetic materials of the cylinder in the pellet carrier.

According to Section II.2.2.2, this calls for a magnetic induction in the coil center of 2.4 T which is generated by a 39 kA current. Further parameter values are listed in Table II.2-4.

Pellet velocity	v	200 m/s
Driving body:		
material		Permendur
density	ρ_f	8.3 g/cm ³
saturation value of magnetic induction	B_c	2.45 T
cylinder radius	r_c	3.5 mm
cylinder length	l_c	7 mm
mass	M_c	2.25 g
Pellet carrier mass (material: plastic)	M_T	1.9 g
pellet mass	M_P	0.35 g
projectile mass	M	4.5 g
Ratio of projectile mass to driving body mass	M/M_c	2
Field coils:		
effective gradient of magnetic induction	$\delta_x B$	170 T/m
radius	r_f	1 cm
current intensity (to generate B_o)	I_f	39 kA
magnetic induction in the center of the coil	B_o	2.4 T
coil spacing		1 cm
number of coils		100
Acceleration distance	l_a	1 m
Time of acceleration	t_a	10 ms

Table II.2-4: Reference parameter values for a projectile acceleration to 200 m/s by means of a cylindrical driving body made from Permendur

II.2.3 Superconducting Coil

Since the pellet and the pellet carrier must be brought to a cryogenic temperature prior to injection, use of a superconducting coil mounted to the pellet carrier as a driving body would be an obvious solution. A pellet carrier equipped in this way is then cooled down below the critical temperature of the superconductor in a strong magnetic field prior to injection and loading with the pellet. The current so induced remains resistant and generates a permanent magnetic moment as long as the critical temperature T_c of the superconductor is not surpassed or, at a given temperature below T_c , a certain strength of magnetic induction of an external magnetic field is not exceeded.

II.2.3.1 Acceleration Distance

Setup for the accelerating force:

$$F = \mathcal{M}_s \cdot \delta_x B$$

\mathcal{M}_s : magnetic dipole moment of superconducting driving body coil in $A m^2$

B : magnetic induction of external field coil

$\delta_x B$: gradient of B in the x-direction

The magnetic moment \mathcal{M}_s shall be generated by an circular current I_s in the driving body coil.

$$\mathcal{M}_s = \pi r_s^2 I_s =$$

r_s : radius of superconducting coil

I_s : induced coil current (by flux entrapment)

$$= \frac{M_s r_s J_s}{2 \varrho_s}$$

J_s : current density in the superconducting coil resulting from I_s

ϱ_s : specific density of superconducting material

M_s : mass of superconducting coil

This gives:

Projectile acceleration:

$$a = \frac{M_s r_s J_s \delta_x B}{2 M \rho_s}$$

M: projectile mass
 = $M_s + M_p + M_T$
 (same meaning as in
 Section II.2.2.3)

Acceleration distance:

$$l_a = \frac{v^2}{2a} = v^2 \cdot \frac{M \rho_s}{M_s r_s J_s \delta_x B}$$

For the current density J_s in the superconducting coil an upper limit is set at a given temperature T_s and a given magnetic induction B_{ext} of an external magnetic field: the respective critical current density $j_c(B_{ext}, T_s)$ of the pure superconducting material. In the following considerations we shall put $J_s = a \cdot j_c$. The factor a takes into account the use of multi-filament conductors for the driving body coil and constitutes the ratio of the cross sectional area of the pure superconducting material (filaments) to the cross sectional area of the whole conductor (coil).

In the following paragraphs we shall assume in an approximation that the external magnetic induction acting upon the driving body is not greater than B_0 - which means equal to the magnetic induction in the center of the field coil. This approximation holds if the magnetic induction resulting from the current I_s of the driving body coil is small as compared with B_0 which must be taken into account when choosing B_0 .

Consequently, with $J_s = a \cdot j_s(B_0, T_s)$ and with the approximation $\delta_x B = 0.7 B_0 / r_f$ justified in Section II.2.2.2 we obtain for the acceleration distance:

$$l_a = v^2 \frac{M r_f \rho_s}{M_s r_s 0,7 a j_c(B_0, T_s) B_0}$$

II.2.3.2 Discussion of the Acceleration Distance

The expression above for l_a takes into account coupling of B_o of the external accelerating magnetic field - and hence of the gradient $\delta_x B$ - to the critical current density of the superconductor and thus constitutes a lower limit for the acceleration distance as regards a given choice in favor of the other parameters.

The dependence of the acceleration distance on B_o (or $\delta_x B$) takes a parabolic course. Although at a given temperature of the driving body coil and for small values of B_o high current densities are possible, the gradient $\delta_x B$ of the field coils is rather weak. On the other hand, high gradients $\delta_x B$ also call for high B_o -values so that the permissible critical current density j_c becomes correspondingly low. In both cases, the acceleration distance increases to a similarly high extent.

For the quantitative evaluation NbTi is used as the superconductor for the driving body coil. Present work on superconductor development is aimed at the construction of superconducting magnets for application in the highest possible (critical) magnetic fields. The commercial superconductors are normally in the form of filaments with copper and aluminium for cryostatic and mechanical stabilization. The mechanical loading resulting from the pinning force density $j_c B_o$ can be estimated from a corresponding mechanical stress $\sigma = j_c B_o r_s$ where r_s is the radius of the driving body coil. The pinning force density for NbTi containing 46.5 wt.% Ti has a maximum value of about 9×10^9 N/m³ for 4.2 K; see Fig. II.2-4 [7]. This gives for $r_s = 3$ mm the value $\sigma = 3 \times 10^7$ N/m². It is still by about one order of magnitude below the tensile strength of pure NbTi (46 wt.% Ti) of

about 4×10^8 N/m² /16/. Nevertheless, at least one material must be available for cryostatic stabilization since the upper limit of the diameter for an electrically inherently stable NbTi conductor is about 50 μ m.

In the subsequent considerations a driving body coil made from an NbTi conductor with copper for cryostatic stabilization is considered, assuming that $a = 0.5$. The mean specific density ρ_s is about 7.5 g/cm³ provided that NbTi with 46.5 wt.% Ti (density 6 g/m³) is used. If one chooses $r_s = 3$ mm and a coil cross section $q_s = 3$ mm², the driving body coil has a mass $M_s = 0.4$ g. Let 1.3 g be the sum of pellet carrier mass and pellet mass; we then obtain $M = 1.7$ g, i.e., $M/M_s \approx 4$.

These parameter values and the data from Fig. II.2-4 according to [7] form the basis of the plots entered in Fig. II.2-5 where the field coil radius r_f is 10 mm and the pellet reference velocity is 200 m/s [1]. For the application in question it must be taken into account that the driving body coil during acceleration is heated by friction heat which is transmitted to the pellet carrier. The development of the temperature of the driving body coil in the course of acceleration cannot be assessed here because it depends on the special geometry, the material and the initial temperature of the pellet carrier as well as on the efficiency of guide tube cooling. Plots (1) and (2) of Fig. II.2-5 reveal however the relative influence exerted by the temperature^{*)} of the driving body coil on the acceleration distance. Upon transition from 4.2 K to 7 K the minimum acceleration distance increases by approximately a factor 3; moreover, at 7 K the margin B_o and $\delta_x B$, respectively, is relatively low with a short acceleration distance as compared with the plot obtained at 4.2 K.

*) The critical temperature T_c of the superconductor constitutes an upper limit to the temperature of the driving body coil; T_c (NbTi) = 0.5 K.

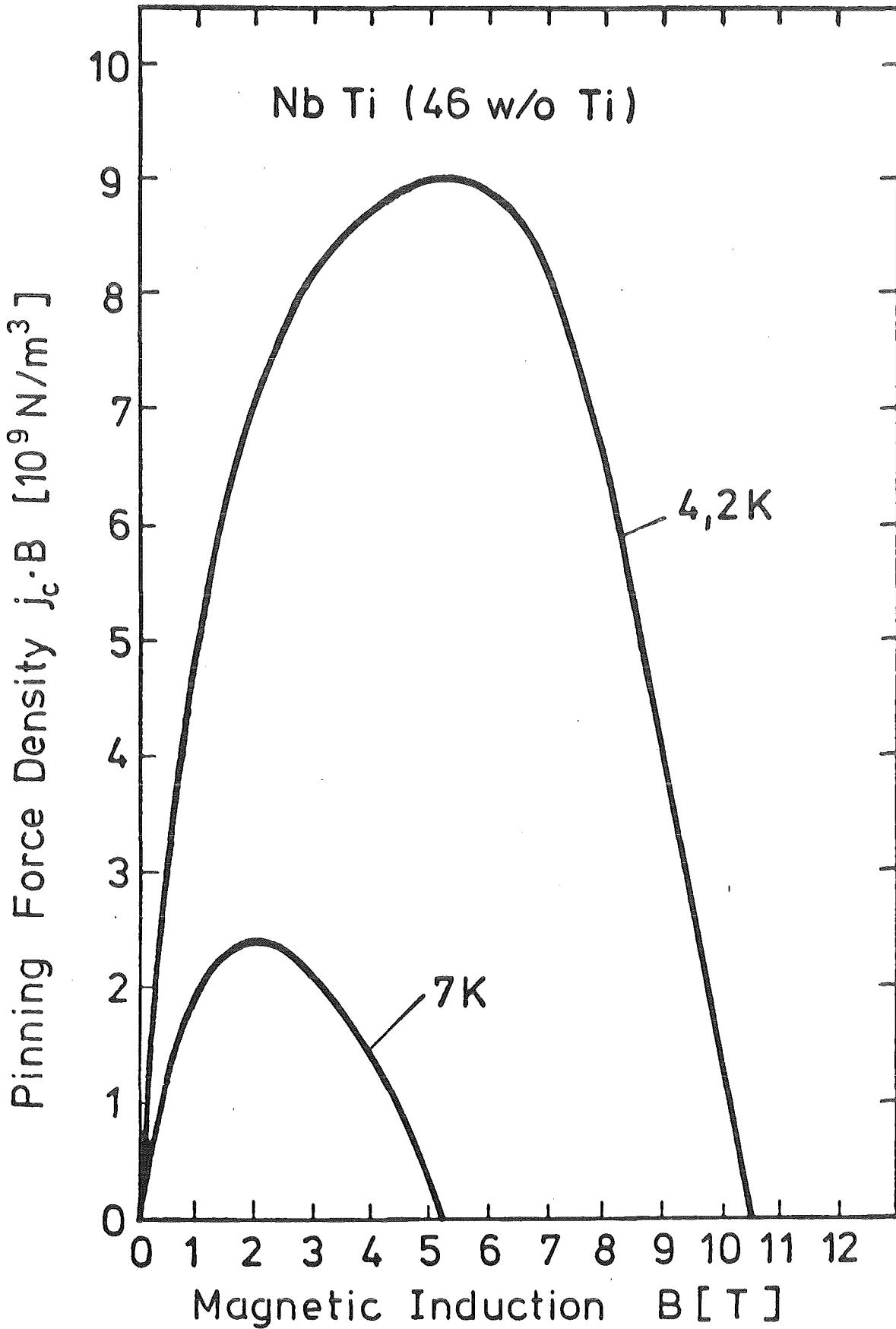


Fig. II.2-4: Pinning force densities for NbTi [7].

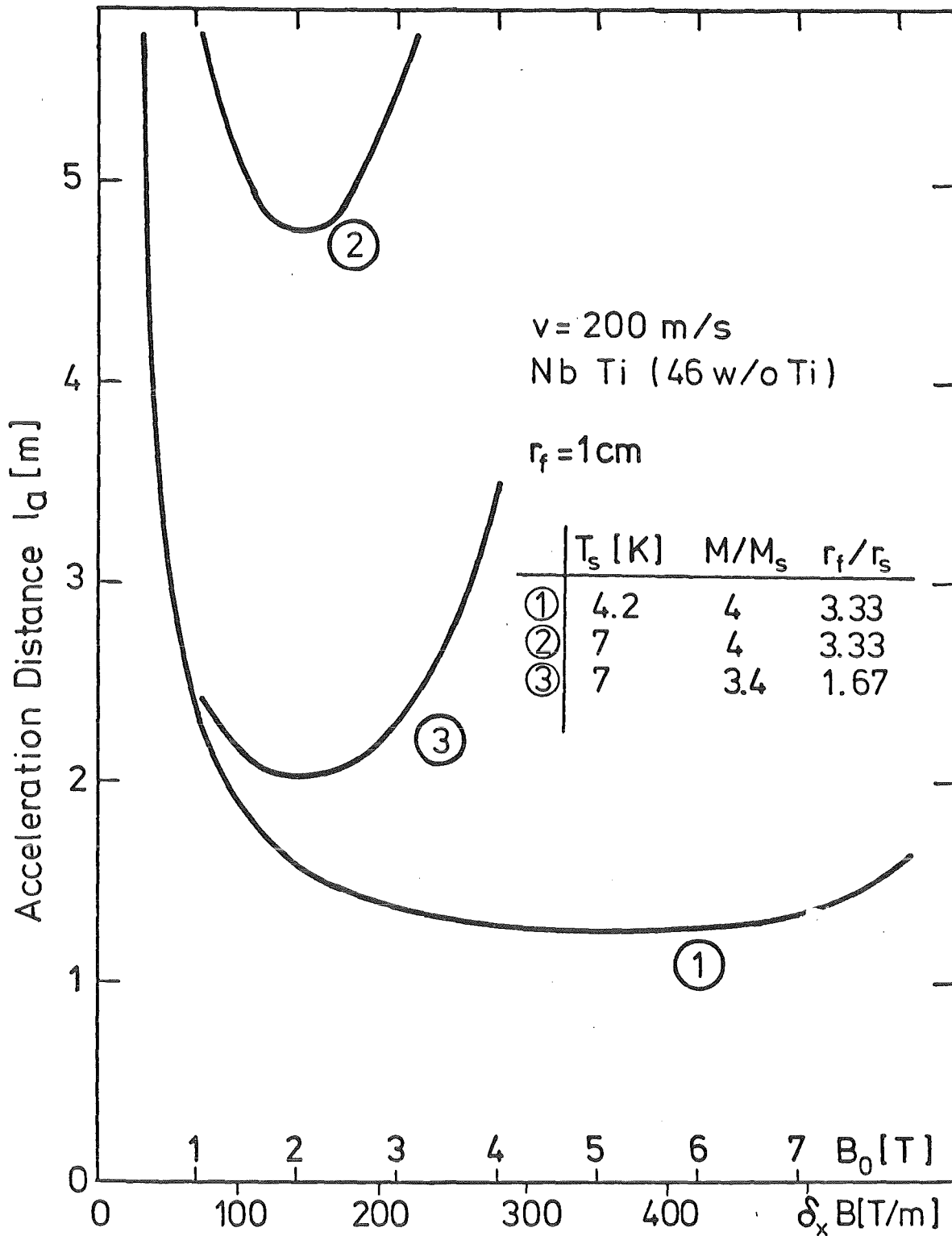


Fig. II.2-5: Acceleration distance as a function of the gradient $\delta_x B$ of magnetic induction of the accelerating magnetic field for the driving body coil of an NbTi superconductor; B_0 : magnetic induction in the center of the field coil; coupling of the ordinate scales by $\delta_x B = 0.7 B_0 / 1 \text{ cm}$.

Also optimization, i.e., minimization of $M/(M_s r_s)$ can contribute to reducing the acceleration distance. For instance, in relation to the case above ($M/M_s = 4$ and $r_s = 3$ mm) a factor 2.4 can be obtained by increasing the radius of the driving body coil. For $r_s = 6$ mm (and $q_s = 3$ mm²) we obtain $M_s = 0.85$ g. On account of the greater coil radius a greater pellet carrier mass is specified; supposing $M_T + M_P = 2$ g, and hence $M/M_s = 3.4$, we obtain:

$$\frac{\left(\frac{M}{M_s r_s}\right) \text{ 1. example}}{\left(\frac{M}{M_s r_s}\right) \text{ 2. example}} = \frac{1.33}{0.56} = 2.4$$

Using the values for pellet carrier design according to the second example and the pinning force densities at 7 K, we obtain plot (3) in Fig. II.2-5.

Use of a type II superconductor such as e.g., Nb₃Sn allows to accommodate higher pinning force densities than will NbTi. According to [8] the $j_c B$ values for Nb₃Sn-filament conductors are higher by a factor 4 to 6 than the values for NbTi as used above which means a corresponding reduction of the acceleration distance. As a matter of fact, Nb₃Sn has less strength than NbTi so that more material might be needed for mechanical stabilization of the driving body coil, i.e., the cross sectional ratio a should, accordingly, be chosen less than 0.5 - as in the case of NbTi. Another advantage of using Nb₃Sn lies in its higher critical temperature of 18.4 K as compared to NbTi with $T_c = 9.5$ K.

II.2.3.3 Reference Parameters

For the set of reference parameters in Table II.2-5 NbTi was selected as the superconducting material for the driving body coil. A reference temperature T_s of the driving body coil of 4.2 K was chosen. For the application intended here it is then reasonable to cool down the pellet carrier (and the pellet) to a temperature below 4.2 K before introducing it into the accelerating tube because in any case friction heat is transmitted to the pellet carrier in the course of acceleration. It is then assumed that by sufficient cooling and by evacuation of the accelerating tube combined with a suitable design of the pellet carrier, the driving body coil is not heated up well above 4 K. This is also a requirement resulting from the consistency with the previous HIBALL scenario for pellet injection [1] since, particularly for calculating pellet heating up during its flight through the reactor chamber, an initial pellet temperature of 4 K was assumed which allows to choose a pellet velocity of not more than 200 m/s.

For the ratio of projectile mass to mass of the driving body coil the use of a suitable plastic material is assumed with a low heat conductivity and a low friction coefficient in contact with the accelerator tube material (volume of pellet carrier material about 1 cm^3) so that a ratio M/M_s of 4 becomes possible for a radius of 3 mm and a conductor cross section of 3 mm^2 of the driving body coil.

Since the pellet carrier is to be accelerated by pulling it into the magnetic field of each field coil, the magnetic field of the field coil and the magnetic field inherent in the driving body overlap within the driving body coil, both running in the same direction. Parametrization of the acceleration distance over j_c as a function of B_0 , as described above,

requires that the magnetic field inherent in the driving body is small against B_0 . This is e.g., the case for $B_0 = 5$ T since at $j_c(5 \text{ T}, 4.2 \text{ K}) = 1.8 \times 10^9 \text{ A/m}^2$ - according to Fig. II.2-4 - and with the dimensions chosen according to Table II.2-5 a magnetic induction of about 0.6 T is obtained in the center of the driving body coil which is small as compared with $B_0 = 5$ T. Consequently, field coils are chosen with a magnetic induction in the coil center of 5 T and a radius of 1 cm. If the coils are arranged at 1 cm spacing an acceleration distance of 1.27 m (127 coils) is obtained so that a pellet velocity of 200 m/s is possible for a mass ratio M/M_s of 4. The mean effective gradient as regards acceleration $\delta_x B$ is 350 T/m.

Pellet velocity	v	200 m/s
Superconducting driving body coil:		
material		NbTi/copper
density (mean)	ρ_s	7.5 g/cm ³
radius	r_s	3 mm
cross section	q_s	3 mm ²
cross sectional ratio (superconductor material to q_s)	a	0.5
mass	M_s	0.4 g
temperature	T_s	4.2 K
critical current density at B_o, T_s	j_c	1.8 x 10 ⁹ A/m ²
current intensity (across conductor cross section)	I_s	2.7 kA
Pellet carrier mass (material: plastic)	M_T	1.0 g
pellet mass	M_P	0.3 g
projectile mass	M	1.7 g
Ratio of projectile mass to driving body coil mass	M/M_s	4
Field coils:		
gradient of magnetic induction	$\delta_x B$	350 T/m
radius	r_f	1 cm
current intensity (to generate B_o)	I_f	80 kA
magnetic induction in the center of the coil	B_o	5 T
coil spacing		1 cm
number of coils		127
Acceleration distance	l_a	1,27 m
Time of acceleration	t_a	13 ms

Table II.2-5: Reference parameter values for a projectile acceleration to 200 m/s by means of a superconducting coil as a driving body

II.3 Types of Accelerator

In the following paragraphs two concepts will be described for the accelerator of an electromagnetic pellet injection system. Both design versions have in common that the pellet carrier (with the pellet embedded) runs in a tube while being accelerated, around which coils and coil loops, respectively, are provided in order to generate the accelerating magnetic field.

Regarding the overall concept of an electromagnetic pellet injection system it is reasonable to slow down the pellet carrier behind the accelerator through a coil system designed on the same principle so that the pellet carrier can be reused.

II.3.1 Single Coil Operation

If a set of individual coils is provided to accelerate the pellet carrier, the coils by a suitable electric circuit must successively be supplied with currents in synchronism with the movement of the pellet carrier. Fig. II.3-1 shows schematically the design of the accelerator tube with a pellet carrier; the example selected of the driving body was a ferromagnetic cylinder with a magnetic moment.

Each field coil is operated with a rectangular current pulse which is always triggered when the front of the driving body is at a distance r_f in front of the field coil for the next respective acceleration step; from this point of time, the acceleration over a length corresponding to the size of the coil radius r_f is proportional to a gradient $\delta_x B$ of the order B_0/r_f ; see Section II.2.2.2. The reference parameter sets in Tables II.2-4 and II.2-6 apply to such an operational mode of the accelerator coils.

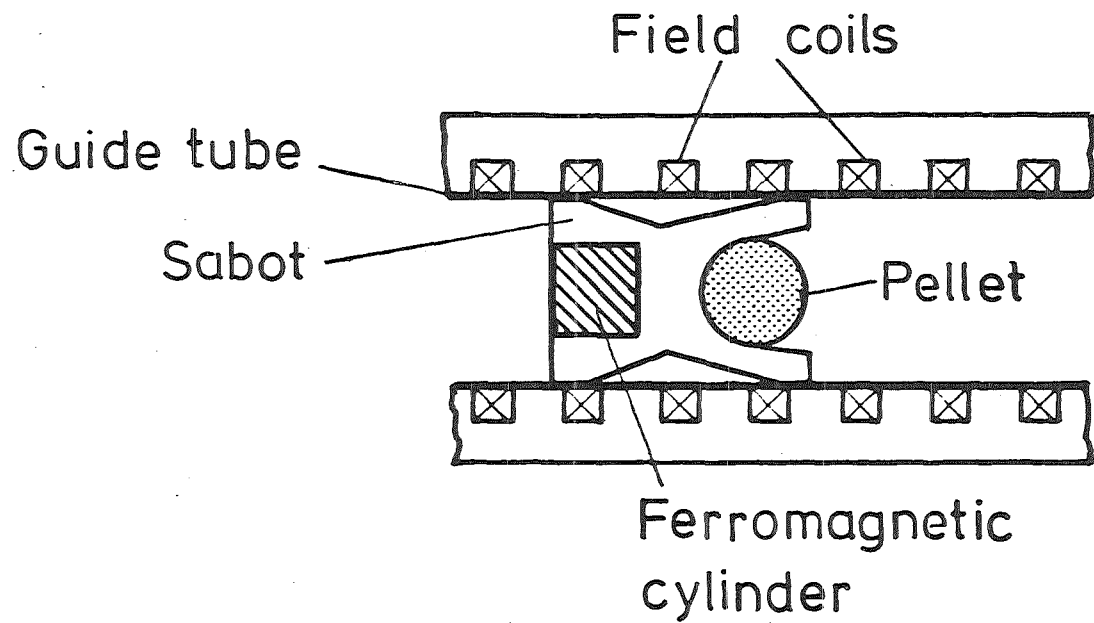


Fig. II.3-1: Longitudinal section of an accelerator for electromagnetic pellet acceleration (schematic).

The rise time of the field coil current shall be small compared with the acceleration time Δt_f between two field coils. Δt_f , for a coil spacing of 1 cm and a projectile velocity of 200 m/s, adopts the value of 50 μ s. This means that the rise time in the zone where the last coils are installed, should attain the order of magnitude of 1 μ s. This value is to be realized e.g., also for the rise time of the magnetic field of kicker magnets of the heavy ion driver of HIBALL-I [1].

Given the high currents, it is appropriate to feed the individual coils via capacitors which are charged prior to acceleration and connected, after the onset of acceleration, in synchronism with the projectile movement of the respective coil. The time of connection can e.g., be triggered individually for each field coil by means of a laser barrier (see estimates on pellet trajectory tracking in [1]).

In case it is considered to operate with alternating current the operating principle of a synchronous motor offers itself as a solution. Here the driving body with the magnetic moment takes over the role of the pole wheel of a synchronous motor. In case three-phase-AC is supplied, each third field coil of the pellet accelerator would be operated with the same current phase. The speed of a synchronous motor (after the startup phase) is directly proportional to the frequency of the alternating current of the field coils. Extrapolated to the pellet accelerator this means that the pellet velocity can be set via the frequency of the field coil current. To shorten the acceleration distance, the pellet carrier could be equipped with two or several driving bodies also whose spacing corresponds to that of field coils actuated in phases; cf. also [9].

II.3.2 Traveling Magnetic Wave Accelerator

II.3.2.1 Functioning Principle

This type of accelerator is based on a proposal made by Winterberg [10] for launching projectiles to hypervelocities (order of magnitude 100 km/s).

The accelerator essentially consists of an elongated coil in a current circuit with main current supply system. The coil turns are fed with additional current pulses in synchronism with the movement of the accelerated projectile via capacitors using auxiliary current sources; see Figs. II.3-2 and II.3.3 (spacing of turns approximately corresponding to the size of the coil diameter). This is necessary if one wishes to achieve a constant acceleration of the projectile since the current pulse of the main current source decreases exponentially with the time when passing through the coil. The trigger pulse connecting the individual auxiliary current sources to the relevant coil turns via a command cable must be delayed to conform to the projectile motion.

A quantitative treatment especially for the application of impact fusion has been described in [2, 15].

II.3.2.2 Accelerator Scheme

Fig. II.3-4 shows a structural scheme of a traveling magnetic wave accelerator [2]. The projectile guide tube around which the accelerator coil is wound together with the capacitors belonging to each coil turn have been embedded in an insulating material which fills up the external housing with the evacuated wall. Provisions must be made that the projectile guide tube of the accelerator remains refrigerated at cryogenic temperatures when used for pellet injection. Further details on accelerator operation, especially on the current supply to coil turns from auxiliary current sources, can be taken from [2].

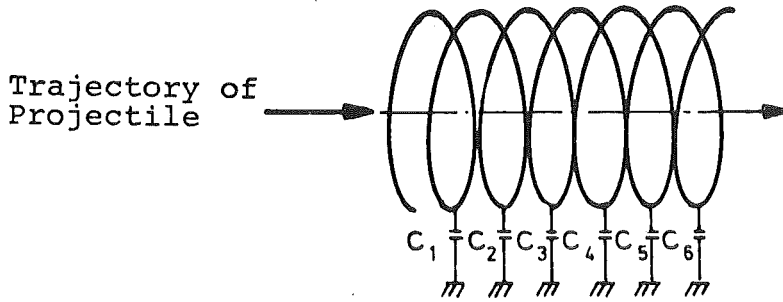
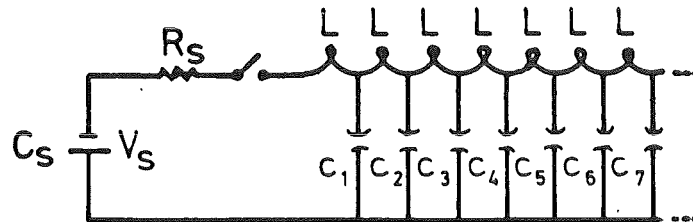
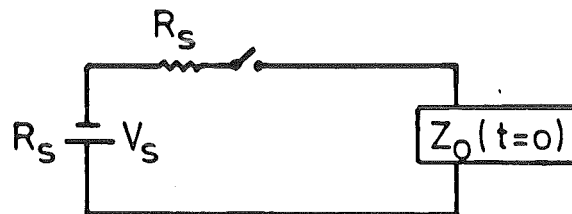


Fig. II.3-2: Principle of a traveling magnetic wave accelerator.

(a)



(b)



$$I_s(t) = I_0 \exp(-t/\tau_s)$$

$$\tau_s = C_s [R_s + Z_0(t=0)]$$

$$Z_0(t=0) = (L/C_1)^{1/2}$$

Fig. II.3-3: (a) Source circuit and (b) equivalent circuit for a traveling magnetic wave accelerator /2/

- V_s : source voltage
- C_s : source capacity
- R_s : source resistance
- $Z_0(t=0)$: initial characteristic impedance of accelerator
- C_1 : capacity of first accelerator capacitor
- L : self-induction of coil turn
- τ_s : time constant for exponential reduction of source current
- I_0 : initial source current

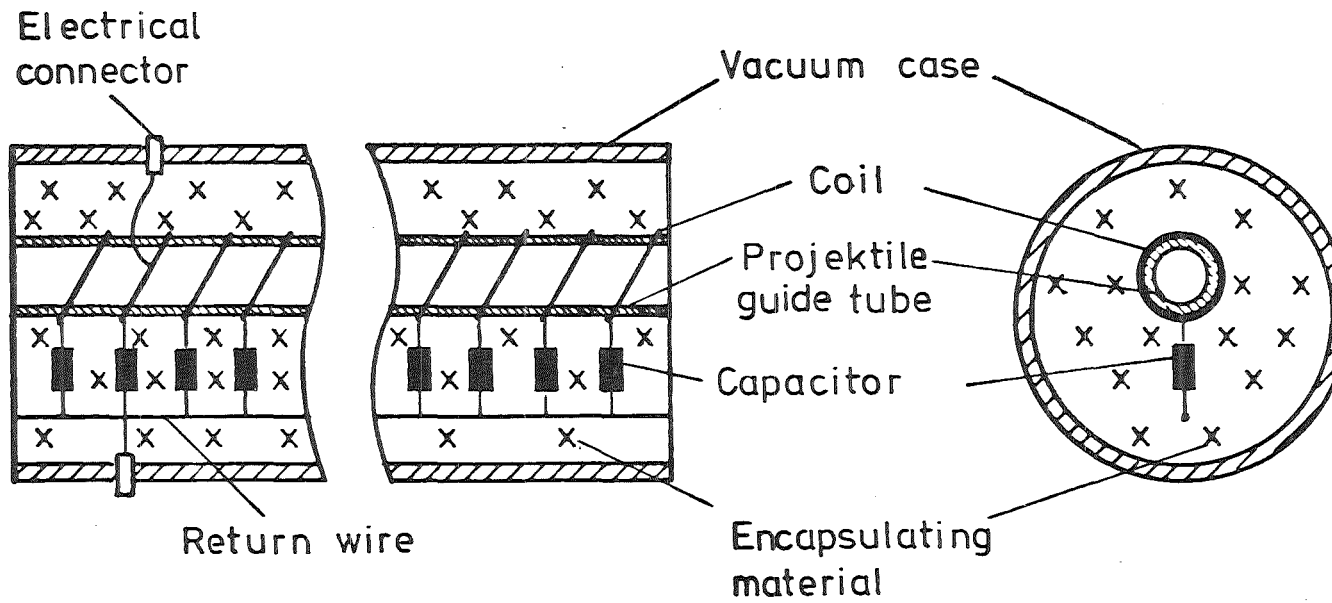


Fig. II.3-4: Structural scheme of a traveling magnetic wave accelerator [2].

II.3.2.3 Energy Stored per Coil Turn

Setup for E_L :

$$E_L = \frac{L_f}{2} I_f^2$$

E_f = energy stored per coil turn

I_f = coil current

L_f = coil inductivity

Setup for I_f :

$$I_f = \frac{2}{\mu_0} B r_f$$

B = magnetic induction of coil

r_f = radius of coil

Hence:

$$E_L = \frac{2}{\mu_0} L_f B^2 r_f^2$$

Inductivity of a ring loop with radius r_f and conductor radius r_w , if $r_f \gg r_w$ [6]:

$$L_f = 4\pi\mu_0 r_f \cdot \left(\ln \frac{8 r_f}{r_w} - 2 + \mu_r k \right)$$

With $\mu_r k \ll 1$:

$$L_f [10^{-9} \text{H}] \approx 4\pi r_f [\text{cm}] \left(\ln \frac{8 r_f [\text{cm}]}{r_w [\text{cm}]} - 2 \right)$$

Examples:

r_f [cm]	0.5	1	1	2	0.5	1
r_w [cm]	0.05	0.1	0.05	0.1	0.1	0.2
L_f [10^{-9} H]	15	30	38.6	77.3	10.6	21.2

Example:

According to Table II.2-4 a magnetic field is required with a magnetic induction B_0 of 2.4 T and a field coil radius r_f of 1 cm. If one chooses $r_w = 0.2$ cm for the radius of the conductor cross section of the field coil one obtains $L_f = 2.1 \times 10^{-8}$ H for the inductivity of the field coil and, finally, $E_L = 15.4$ J per field coil. For 100 field coils a total energy of 1.54 kJ is needed which corresponds to a mean power of 7.7 kW over 0.2 seconds. Since only a relatively small portion of the coil energy is consumed for projectile acceleration - about 6% in case the values of Table II.2-4 apply - it is appropriate to recover the field coil energy by a suitable electric circuit.

II.4 Conclusion

Acceleration by means of a driving body made from a non-ferromagnetic (electrically conducting) material should be left out of future considerations on account of intrinsic heating of the driving body due to the current induced and on account of the other two more favorable potentials offered by driving bodies discussed in this paper.

With a ferromagnetic cylinder having dimensions as in the reference parameter lists, Table II.2-4 and Table II.2-5, or with an NbTi-superconductor coil as the driving body the reference pellet velocity of 200 m/s can be achieved over acceleration distances of 1 m and 1.3 m, respectively, provided that one defines an effective gradient $\delta_x B$ of the field coils of 170 T/m or 350 T/m. For the field coils a 1 cm radius and spacing are selected. To produce the gradients, a maximum magnetic induction B_0 in the center of the field coils of 2.4 T or 5 T is required which calls for field coil currents of 39 kA and 80 kA, respectively.

It shall be underlined again here that the estimation of the acceleration distance relies on a one-dimensional model. Due to the finite dimensions of the driving body and an accelerator efficiency differing from unity^{*)}, greater acceleration distances must be expected in practical application for the field coil values indicated here unless the field coil parameters as given here are interpreted as the actually effective values for acceleration in the real case. Generally speaking, however, the acceleration distances indicated here should be realistic values within a factor 2 towards higher values.

Thus, it can be stated in general that pellet acceleration by means of a magnetic field with a high gradient fits the previous frame in terms of space and time for pellet injection of HIBALL-I [1]; in other words, that an acceleration distance of the order of 1 m and an acceleration time of about 10 ms are possible in order to obtain pellet velocity of 200 m/s while only moderate requirements are needed for the field coils.

For reasons of technical simplicity a ferromagnetic driving body must ultimately be preferred to a superconducting driving body coil since in the latter case the requirements must be higher as regards pellet carrier design so as to possess measures of effective insulation against the friction heat transmitted to the pellet carrier and to shield the superconductor (normal conducting component) against the external accelerating magnetic field.

^{*)} Brittingham indicates e.g., for a traveling magnetic wave accelerator with a ferromagnetic projectile an efficiency of 75% [2].

III Railgun Accelerator

III.1 Introduction

Application of the railgun accelerator for impact fusion ^{*)} was studied by Hawke [11]. First experimental results are available. According to [12] velocities of 6 km/s have been achieved with polycarbonate projectiles of about 2 g weight.

In the following paragraphs the principle of acceleration and the mode of functioning of a railgun accelerator will be described and the dependence discussed of the acceleration distance on the projectile mass and on the rail current. Rail heating is estimated and a reference parameter set proposed for a railgun accelerator for pellet injection.

III.2 Principle of Acceleration

The acceleration unit of a railgun accelerator consists of two rails in parallel, at the beginning of which a plasma arc is ignited. A current flows through the plasma arc and the rail sections in front of it; see Fig. III.2-1. Due to the interaction of the current in the plasma arc with the magnetic field of the rails the plasma arc moves along the rails while a projectile preceding the plasma arc is accelerated.

The layout of the accelerating tube has been sketched in Fig. III.2-2.

^{*)} Launching macroscopic projectiles to hypervelocities (~ 100 km/s) in order to compress and heat up fusion fuel at the target.

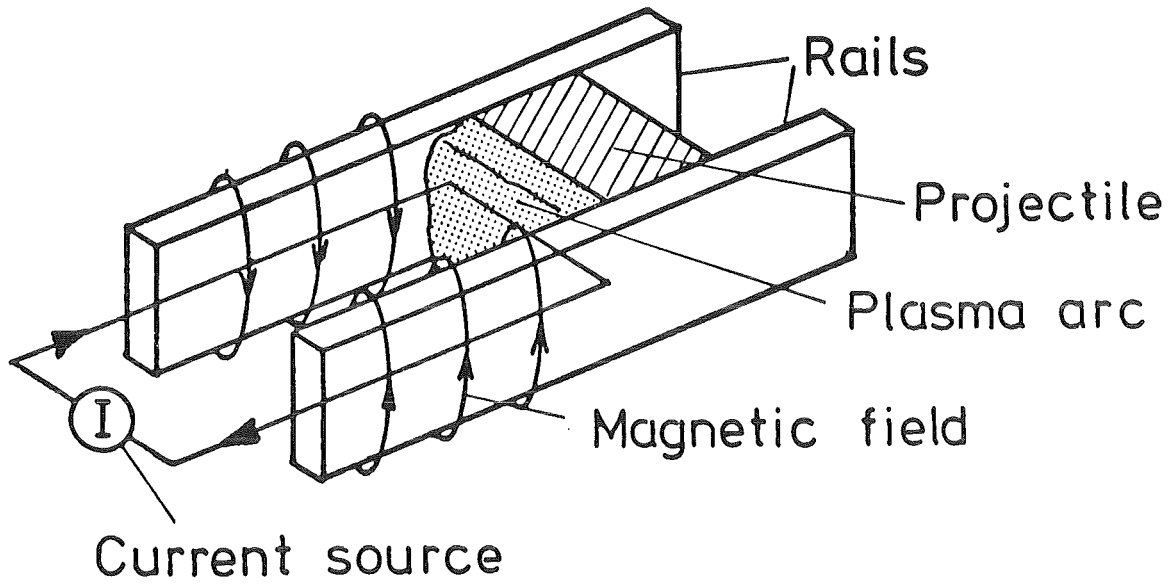


Fig. III.2-1: Principle of acceleration of a railgun accelerator,

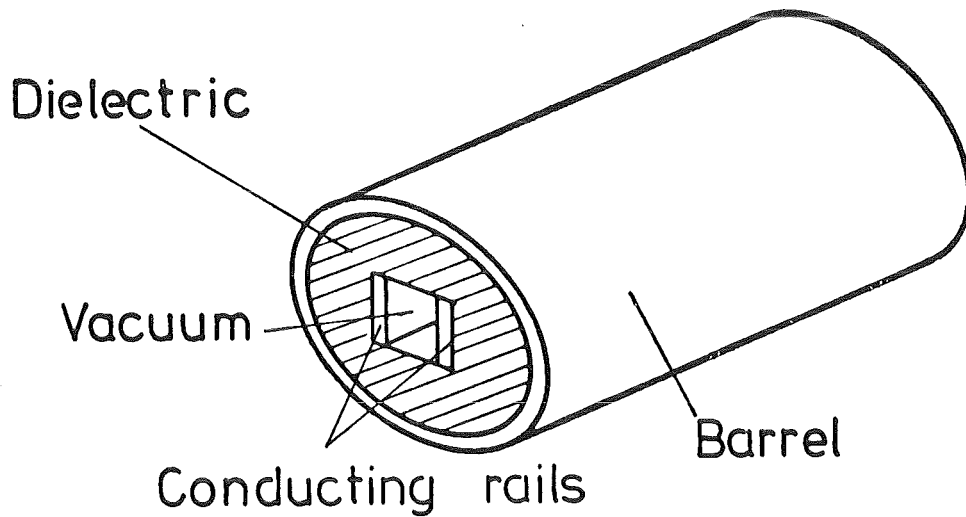


Fig. III.2-2: Layout of accelerating tube of a railgun accelerator.

III.3 Electric Circuit

In the following paragraphs the individual phases of operation of a railgun accelerator will be described by the example of the wiring circuit represented in Fig. III.2-3 [11, 12].

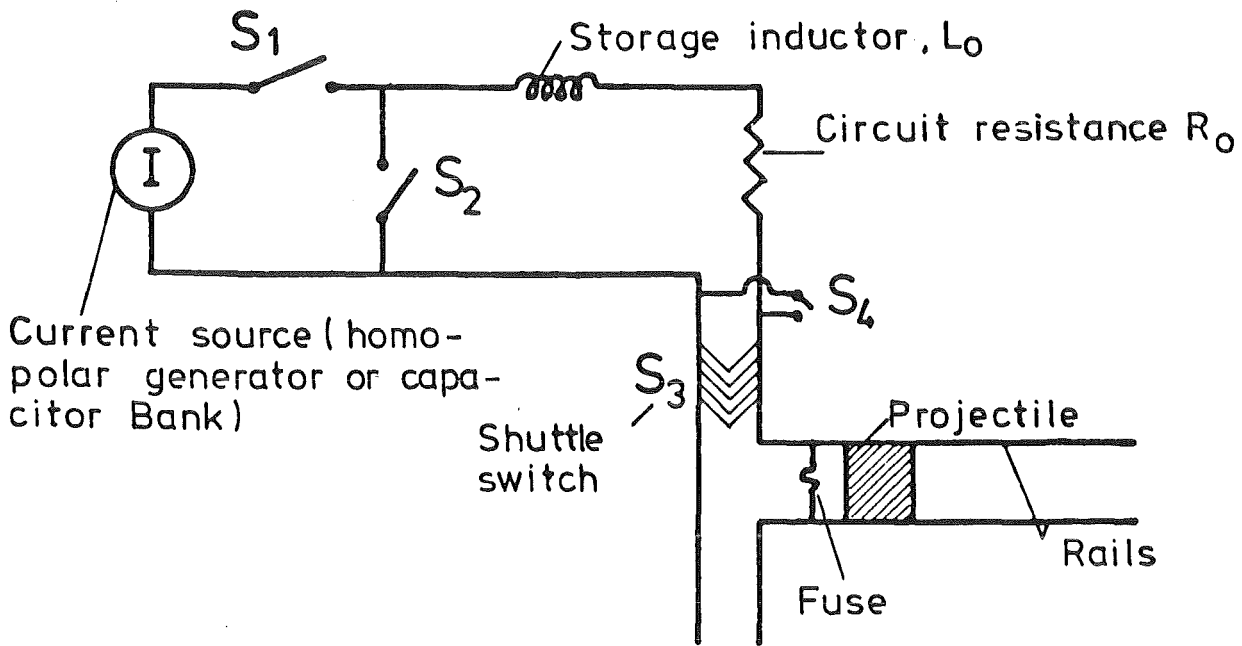


Fig. III.2-3: Wiring scheme of a railgun accelerator.

The power circuit is fed from a homopolar generator or from a capacitor bank . After closure of the switch S_1 the inductance L_0 is recharged. Upon attainment of the maximum (normal case) current S_2 is closed and the current source decoupled in this way from the rest of the current circuit. At the same time, a shuttle switch passes the front end of the railgun. so that a current flows through the fuse provided between the rails. The fuse evaporates and a plasma arc is formed. The plasma arc and the preceding projectile move along the rails. Shortly before attaining the ends of the rails switch S_4 is closed so that the plasma arc is extinguished.

III.4 Projectile Acceleration

Setup for the acceleration pressure [11]:

$$p = \frac{L_1 I^2}{2A}$$

L_1 : inductance (inductive resistance) per unit of length of rails

I : current intensity in the plasma arc

A : cross section of the projectile

Projectile acceleration:

$$a = \frac{L_1 I^2}{2M}$$

M : projectile mass

Acceleration distance:

$$l_a = \frac{v^2}{2a} = \frac{v^2 M}{L_1 I^2}$$

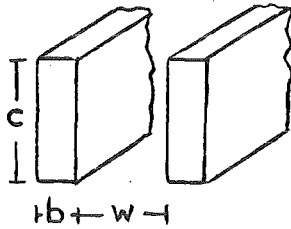
v : projectile velocity

Given the significance of rail inductance L_1 for the acceleration distance, an estimate is first made of L_1 for the eligible rail dimensions.

III.4.1 Inductance of the Railgun

According to [6] the following relation holds for the inductance of two parallel rails of length l with rectangular cross section and distance w , if $l \gg w$:

$$L_1 = \frac{L_0}{l[\text{cm}]} = 4 \cdot 10^{-9} \frac{\text{H}}{\text{cm}} \left(\ln \frac{w}{b+c} + 1.5 - \frac{w}{l} + 0,224 \frac{b+c}{l} \right)$$



Example:

Be $w = c = 1 \text{ cm}$

$$L_1 = 4 \times 10^{-9} \frac{\text{H}}{\text{cm}} \left(\ln \frac{1}{b+1} + 1.5 - \frac{1}{l} + 0.224 \frac{b+1}{l} \right)$$

with b and l expressed in cm.

	l [cm] :	10	100	
b [cm]				} L_1 in $10^{-7} \frac{\text{H}}{\text{m}}$
0.1		5.2	5.5	
0.2		5.0	5.2	
0.3		4.4	4.8	
1.0		2.7	3.2	

It appears from the foregoing table that specifying for b a value between 0.1 and 1 cm and for l between 10 and 100 cm has no major influence on L_1 . Therefore, the characteristic value $L_1 = 5 \times 10^{-7} \text{ H/m}$ is used for calculation in the following.

III.4.2 Acceleration Distance

The following derivation was made:

$$l_a = \frac{v^2}{L_1} \cdot \frac{M}{I^2}$$

For a projectile velocity of 200 m/s and the characteristic value $L_1 = 5 \times 10^{-7}$ H/m (see Section III.4.1) the following specific relation is obtained:

$$l_{a[m]} = 8 \times 10^{10} \frac{A^2 m}{kg} \cdot \frac{M [kg]}{I^2 [A^2]}$$

In Fig. III.4-1 the dependence is shown of the acceleration distance on the rail current for three values of the projectile mass. Accordingly, a projectile mass of 2 g is accelerated by a rail current of 10 kA over 1.6 m length, a mass of 10 g by a rail current of 20 kA over 2 m length to 200 m/s.

The railgun efficiency was not taken into account in the calculation. The experimental acceleration distances obtained according to [12], e. g., fall short of the theoretical values by about 10 to 20 % in accordance with the formula for l_a indicated above.

Finally, in the following section the temperature rise on the rail surface which occurs during acceleration as a result of the rail current is estimated for rail currents up to several 10 kA.

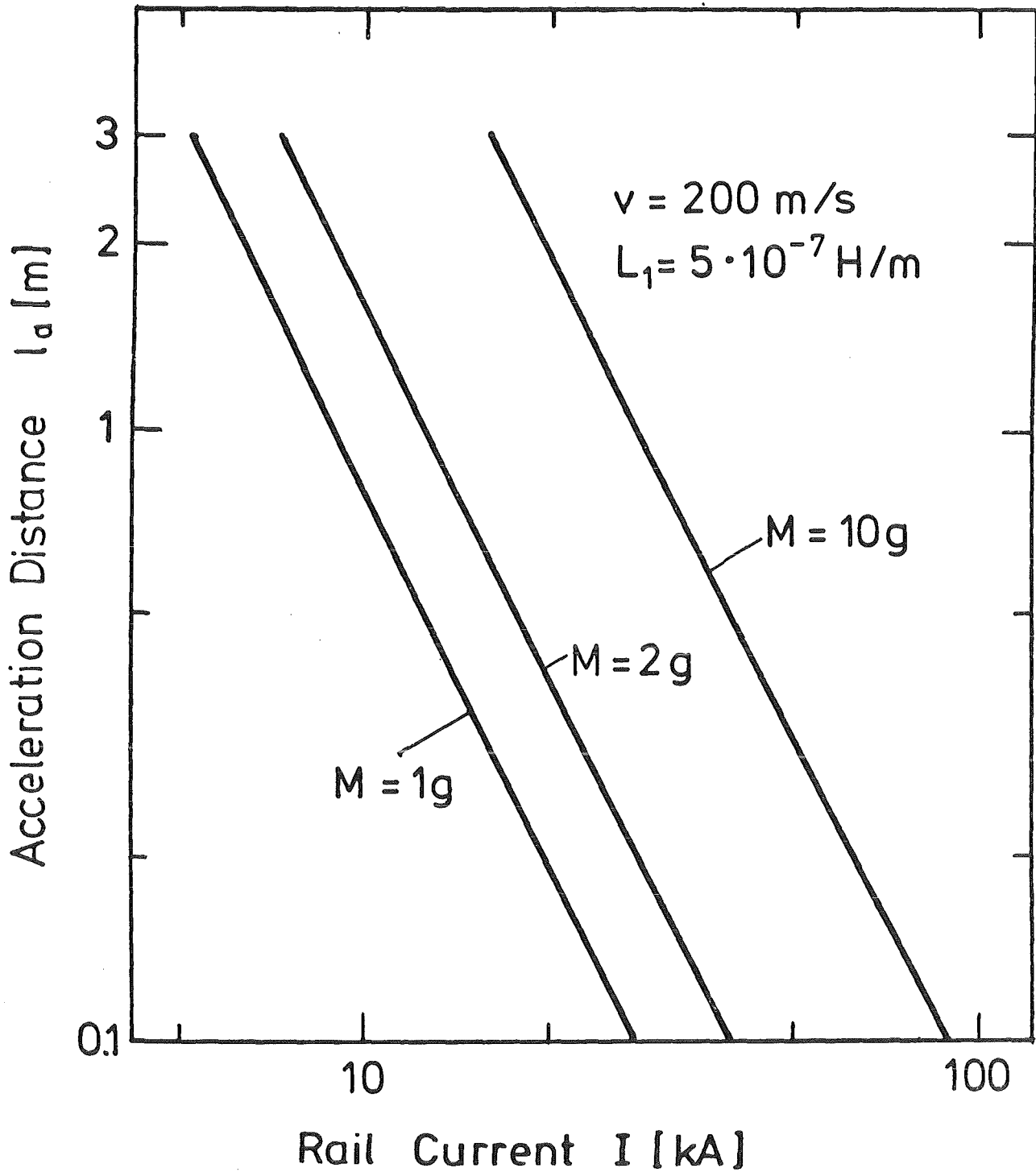


Fig. III.4-1: Acceleration distance for various projectile masses as a function of the rail current of a railgun accelerator.

III.5 Rail Heatup

The maximum temperature occurs on the rail surfaces; the rail current I is a surface current with little skin depth. According to [13] the temperature rise on the surface of a current carrying conductor is in an approximation:

$$\Delta T = \frac{2 \mu_0}{\pi C_v \rho} \frac{I^2}{d^2} \ln \left[1 + \frac{\pi}{2} \left[\frac{C_v \rho \eta_0}{2 \mu_0 k} \right] \right]$$

where

μ_0 = 1.26×10^6 Vs/Am

C_v = specific heat [J/gK].

ρ = specific density [g/cm³]

η_0 = resistivity [Vm/A]

k = specific thermal conductivity [W/cmK]

I = current intensity [A]

d = circumference of conductor cross section (in this context rail cross section) = $2(b + c)$
 (see above)

Introducing the thermal diffusivity α , one obtains:

$$\Delta T = \frac{2 \mu_0}{\pi C_v \rho} \frac{I^2}{d^2} \ln \left[1 + \frac{\pi}{2} \left[\frac{\eta_0}{2 \mu_0 \alpha} \right] \right]$$

This formula applies solely to constant specific heat and specific thermal conductivity, both of them not subjected to changes with temperature, which roughly applies e.g., for copper above 100 K. By contrast, at cryogenic temperatures the thermodynamic variables are greatly dependent on temperature.

In Table III.5-1 the respective thermodynamic and electric data have been entered for copper at 5 and 10 K [3, 6].

T_0 [K]	C_V [$\frac{J}{g \cdot K}$]	α [$\frac{m^2}{s}$]	η_0 [$\frac{V \cdot m}{A}$]
5	8.4×10^{-4}	1.9×10^{-9}	3.15
10	8.4×10^{-5}	1.8×10^{-9}	14.9

Table III.5-1: Thermodynamic and electric data for copper at cryogenic temperatures [3, 6].

If one introduces these values into the formula above for the temperature rise ΔT of the rail surface, one obtains the two plots in Fig. III.5-1 where $\rho = 8.9 \text{ g/cm}^3$ and $d = 3 \text{ cm}$. It results that the values of ΔT for rail currents up to 6.5 kA and an initial temperature $T_0 = 5 \text{ K}$ and up to 20 kA at $T_0 = 10 \text{ K}$ do not exceed 0.05 and 0.1 K, respectively, i.e., they do not attain more than 1% of the initial temperature. This means that at least up to these values of rail current ΔT is so small that the thermodynamic properties undergo relatively small changes. The rail currents of 6.5 kA and 20 kA, respectively, are sufficient to accelerate to 200 m/s, e.g., projectiles of 1 g and 10 g weight, respectively, over a rail length of 2 m; see Fig. III.5-1.

This means that rail heatup for the parameter range of pellet injection considered here is not critical (of the order of 0.1 K).

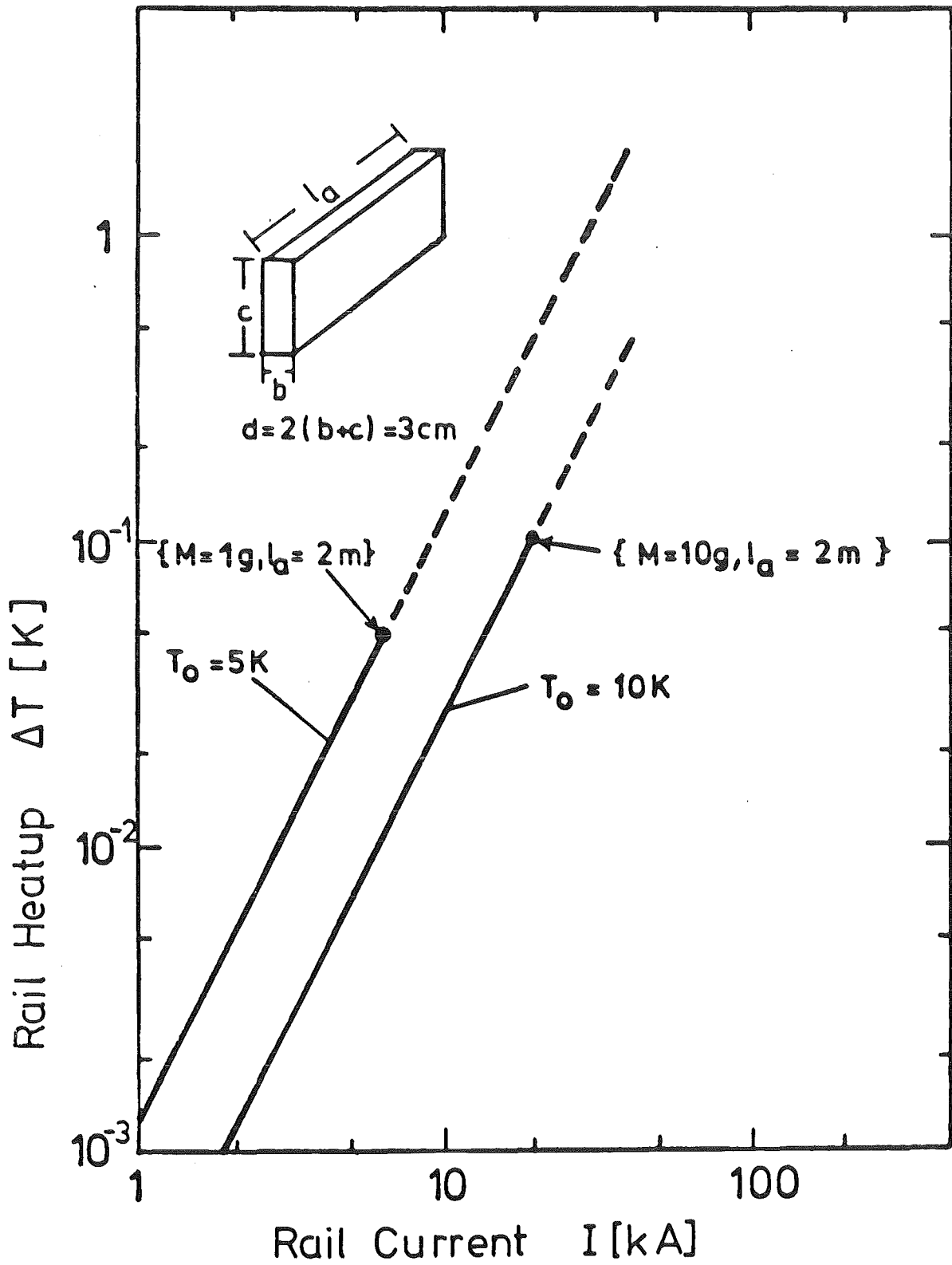


Fig. III.5-1: Rail heatup as a function of rail current for various rail temperatures; dotted line: $T/T_0 \geq 1$

III.6 Reference Parameters

In Table III.5-2 reference parameter values have been entered for launching a 2 g projectile to a velocity of 200 m/s using a railgun accelerator. A rail spacing and a rail height of 1 cm were chosen since reactor-size pellets will be several mm in diameter, e.g., the HIBALL pellet will be 6 mm. The rail thickness is assumed to be 0.5 cm and the rail length 1 m so that a rail inductance of about 5×10^{-7} H/m is obtained and a rail current of 12.6 kA is required in order to accelerate the projectile to 200 m/s.

Pellet velocity	v	200 m/s
Rails:		
rail spacing	w	1 cm
rail thickness	b	0.5 cm
rail height	c	1 cm
rail length (acceleration distance)	l_a	1 m
rail inductance	L_1	5×10^{-7} H/m
rail current intensity	I	12.6 kA
Projectile:		
projectile mass	M	2 g
e.g.,		
pellet mass		0.4 g
sabot mass		1.6 g
sabot material (density ~ 1 g/cm ³)		plastic product

Table III.5-2: Reference parameter values for a projectile acceleration to 200 m/s using a railgun accelerator

Acknowledgment:

The author thanks Dipl. Phys. F. Arendt (ITP) for some useful discussions.

References

- / 1 / B. Badger, et al, "HIBALL - A Heavy Ion Beam Fusion Conceptual Reactor Design Study", KfK-3202 (1981).
- / 2 / J. N. Brittingham, Devices for Launching 0.1 g Projectiles to 150 km/s or more to Initiate Fusion, Part I: Magnetic Gradient and Electrostatic Accelerators, Atomkern-energie. Kerntechnik 36 (1980) 130.
- / 3 / Y. S. Touloukian, R. W. Powell, C. Y. Ho, M. C. Nicolaou, Thermophysical Properties of Matter, Vol. 4, Vol. 10, New York-Washington (1973).
- / 4 / I. Wolf, "Grundlagen und Anwendungen der Maxwell'schen Theorie II", BI-Hochschulschriften, Mannheim (1970).
- / 5 / Handbook of Chemistry and Physics 62, CRS Press, Boca Roton, Florida (1981).
- / 6 / M. von Ardenne, Tabellen zur angewandten Physik, Band III, VEB Deutscher Verlag der Wissenschaften, Berlin (1973).
- / 7 / C. R. Spencer, P. A. Sanger, M. Young, IEEE Transactions on Magnetism, 15, 1 (1979) 76.
- / 8 / W. Schauer, F. Zimmermann, Adv. Cryog. Eng. Mat. 26 (1980) 432.

- / 9 / E. W. Sufov, et al., Inertial Confinement Fusion Central-Station Electric-Power-Generating Plant, Final report for the period March 1, 1979 - September 30, 1980, Vol. 1, WEPS-TME-81-001, (1981).
- / 10 / F. Winterberg, Magnetic Acceleration of a Superconducting Solenoid to Hypervelocities, Plasma Phys.-J. Nucl. Energy, Part C, 8 (1966) 541.
- / 11 / R. S. Hawke, Devices for Launching 0.1g-Projectiles to 150 km/s or more to Initiate Fusion, Part II: Railgun Accelerators, Atom-energie . Kerntechnik 38 (1981) 35.
- / 12 / S. C. Rayleigh, R. A. Marshall, Electromagnetic Acceleration of Macroparticles to High Velocities, J. Appl. Phys. 49 (1978) 2540.
- / 13 / H. Knoepfel, Pulsed High Magnetic Fields, p. 80, North Holland Publ. Co., Amsterdam (1970).
- / 14 / H. S. Carslaw, J. C. Jaeger, Conduction of Heat in Solids, Clarendon Press, Oxford (1959).
- / 15 / F. Arendt, persönliche Mitteilung (1979).
- / 16 / Gmelins Handbuch der anorganischen Chemie, 49, B2, Niob, Verlag Chemie, Weinheim/Bergstraße (1971).